*SAE TECHNICAL PAPER SERIES*

**2007-01-0656**

# Performance Evaluations of Aluminum Titanate Diesel Particulate Filters

**R. S. Ingram-Ogunwumi, Q. Dong, T. A. Murrin, R. Y. Bhargava, J. L. Warkins and A. K. Heibel**
Corning Incorporated

**Reprinted From: Diesel Exhaust Emission Control, 2007 (SP-2080)**

ISBN 0-7680-1635-5

9 780768 016352

**2007 World Congress
Detroit, Michigan
April 16-19, 2007**

SAE International™

400 Commonwealth Drive, Warrendale, PA 15096-0001 U.S.A. Tel: (724) 776-4841 Fax: (724) 776-0790 Web: www.sae.org


*All SAE papers, standards, and selected books are abstracted and indexed in the Global Mobility Database.*



**ISSN 0148-7191**


**Printed in USA**

2007-01-0656

# Performance Evaluations of Aluminum Titanate Diesel Particulate Filters

**R. S. Ingram-Ogunwumi, Q. Dong, T. A. Murrin, R. Y. Bhargava, J. L. Warkins and A. K. Heibel**
Corning Incorporated



## ABSTRACT

Over the past decade, regulations for mobile source emissions have become more stringent thus, requiring advances in emissions systems to comply with the new standards. For the popular diesel powered passenger cars particularly in Europe, diesel particulate filters (DPFs) have been integrated to control particulate matter (PM) emissions. Corning Incorporated has developed a new proprietary aluminum titanate-based material for filter use in passenger car diesel applications. Aluminum titanate (hereafter referred to as AT) filters were launched commercially in the fall of 2005 and have been equipped on more than several hundred thousand European passenger vehicles. Due to their outstanding durability, filtration efficiency and pressure drop attributes, AT filters are an excellent fit for demanding applications in passenger cars.

Extensive testing was conducted on engine to evaluate the survivability and long-term thermo-mechanical durability of AT filters. Catalyzed filters were first tested to failure under severe uncontrolled regenerations to define filter survivability limits by means of filter maximum temperatures and thermal gradients. In the second phase filter durability was evaluated, exposing the AT filter to hundreds of high temperature regenerations. This paper demonstrates a broad window of operation for AT filters under extreme exposures. Furthermore the pressure drop as well as the filtration performance of the filters was investigated and compared to commercially available filter alternatives.

## INTRODUCTION

Today's regulations for diesel passenger car emissions have tightened significantly. It is evident that a wall-flow filter is necessary in order to meet such challenging standards. Use of diesel particulate filters has been the primary approach for particulate matter reduction. The key performance attributes of a viable DPF are low pressure drop, high filtration efficiency, and good thermal durability. The high heat capacity of AT filters is advantageous during thermal regenerations, providing significant durability benefits. Safe filter regeneration, where filter bed temperatures and thermal stresses are maintained at moderate levels, is critical to ensure thermal durability. OEMs are working to improve filter regeneration strategies to provide more control of regeneration conditions. In the interim uncontrolled regenerations, where exhaust flow rates are low and inlet DPF oxygen levels are high, continue to be a challenging condition for filter survival.

High filter pressure drop levels are unattractive due to increased fuel consumption from more frequent regenerations. The AT filter has an asymmetric cell design where the inlet channels are larger than the outlet channels and filtration area is larger than that of the standard cell design. This filter design enables increased soot and ash storage capacity for the same pressure drop as compared to a standard cell geometry filter [1]. In addition, enhanced ash storage capacity of an asymmetric design allows use of a smaller filter.

This study describes the engine dynamometer results of AT filters for pressure drop, filtration efficiency, thermal survivability and durability. Details are provided on the maximum temperatures and thermal gradients observed for AT filters which survive durability tests. In addition, the impact of engine exposure on filter physical properties is discussed.

## EXPERIMENTAL SETUP

Performance evaluations of AT filters were conducted in three separate studies as i) pressure drop and filtration efficiency ii) thermal survivability and iii) thermal durability. These studies were performed concurrently; thus, different engine test benches were used. As shown in Table 1, pressure drop, filtration performance and thermal survivability tests were conducted on a VW 2.0l TDI engine with catalyzed filter installed in the close-coupled position, whereas a Mercedes 2.2l CDI engine was used for durability studies. More detail on engine specifications is included in Table 1.

Table 1. Engine Specifications for Performance Studies

| | Performance Study | |
|---|---|---|
| | Pressure Drop/ Filtration Efficiency/ Thermal Survivability | Thermal Durability |
| Engine Manufacturer | Volkswagen | Mercedes |
| Engine Type | 4 cylinder inline-TC with cooled EGR | 4 cylinder inline-TC with cooled EGR |
| Displacement | 2.0l | 2.2l |
| Rated Power | 103 kW @ 4000 rpm | 110 kW @ 4000 rpm |
| Peak Torque | 330 Nm @ 2000 rpm | 325 Nm @ 1900 rpm |
| Fuel Injection System | Pump unit injection | Common rail injection |
| ECU | Bosch EDC 16 | Bosch EDC 16 |

An eddy current dynamometer was used with the Mercedes 2.2l engine, whereas an AC dynamometer was coupled to the VW 2.0l engine. A 5.66" x 4" diesel oxidation catalyst (DOC) was installed upstream of a 5.66" x 6" 2.5l DPF in the durability tests with the assembly close-coupled to the engine. North American ultra low sulfur fuel (15 ppm) was used for all tests. Figure 1 shows a schematic representation of the exhaust layout and measurements taken during survivability testing.

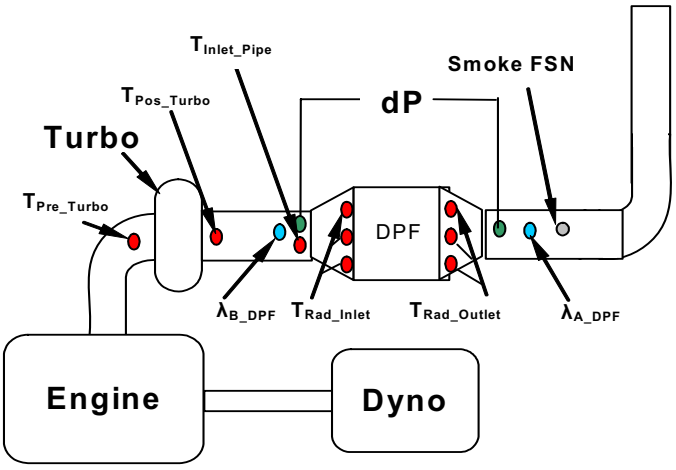


Figure 1. Schematic representation of exhaust layout for thermal survivability, pressure drop and filtration efficiency testing.

DPF pressure loss, exhaust temperatures and lambda before and after DPF were measured. Smoke measurements were made downstream of the DPF using an AVL 415S smoke meter.

A schematic of the exhaust configuration and measurements used during the durability testing is shown in Figure 2. Exhaust temperature before and after the DOC as well as after the filter were monitored. Filter pressure drop was measured using a differential pressure transducer. As a secondary measure absolute pressure before and after the DPF was monitored. During the test, filter integrity was monitored by smoke measurements upstream and downstream of the filter. Oxygen content of the exhaust was measured before and after the DPF using universal exhaust gas oxygen (UEGO) sensors.

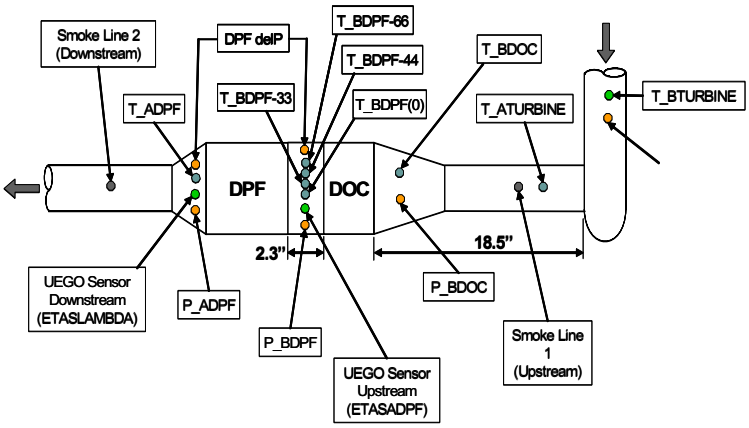


Figure 2. Exhaust configuration for durability evaluations.

Both 5.66" x 6" (diameter x length) and 7.85" x 4" x 6.85" (diameter x diameter x length) filter contours of nominal 300/13 cell geometry were tested in 2.5l and 2.9l volumes, respectively. Table 2 lists the filters and contours evaluated for each performance study. All filters were commercially catalyzed and oven aged prior to engine testing. AT ACT (asymmetric cell technology) samples A-I have a nominal 50% porosity and 17 μm median pore diameter (MPD). Samples were conditioned on engine at full load for 2 hours with a controlled regeneration (using post injection) for the last 15 min. before conducting performance studies.

Table 2. List of Tested Filters for Each Performance Study

| | Sample | Contour (Diam.xDiam.xLength) |
|---|---|---|
| Durability | A | 5.66”x6” |
| | B | 5.66”x6” |
| | C | 5.66”x6” |
| Survivability | D | 7.8”x4” x6.85” |
| | E | 7.8”x4” x6.85” |
| | F | 7.8”x4” x6.85” |
| | G | 7.8”x4” x6.85” |
| dP & Filtration | H | 7.8”x4” x6.85” |
| | I | 7.8”x4” x6.85” |
| | SiC | 7.8”x4” x6.85” |

*Samples A-I are AT ACT

All filters tested for durability were of a round configuration (for ease of installation with Mercedes engine and exhaust layout), whereas those tested for survivability, pressure drop and filtration were an oval shape (specific for customer application). All filters in Table 2 were zone coated with identical washcoat loadings. A commercially available, high porosity, silicon carbide (SiC) 300/12 filter with a commercially applied catalyst with integral DOC function was used as a comparison for the dP and filtration study due to its identical contour volume and catalyst loading.

In order to assess filter thermal profiles during regeneration, up to 24 type K thermocouples were installed in round filters from the filter outlet and 44 in the oval filters. Figures 3 and 4 show the thermocouple patterns for round and oval filters, respectively. The thermocouples at the filter outlet near the center and those at the periphery were spaced ~10mm apart in order to capture the maximum temperature and maximum gradients. Thermocouples were placed in axisymmetric locations to monitor uniformity of thermal profiles around the filter azimuth. For example, thermocouples 20, 22, and 24 in Figure 3 are located at the same axial and radial positions but a different azimuth. Since the oval filter is not symmetric, thermocouples were located at axisymmetric positions at the inlet, middle and outlet of filter as shown in Figure 4.

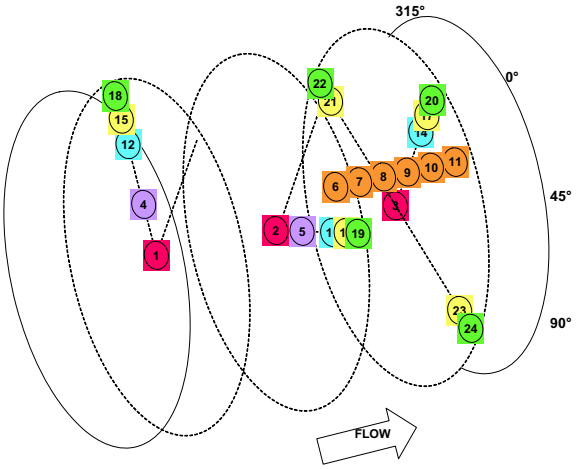


| TC No. | Coordinates Axial mm | Radial mm | Azimuth deg |
|---|---|---|---|
| 1 | 25 | 0 | 315 |
| 2 | 75 | 0 | 45 |
| 3 | 125 | 0 | 0 |
| 4 | 25 | 22 | 315 |
| 5 | 75 | 22 | 45 |
| 6 | 95 | 22 | 0 |
| 7 | 105 | 22 | 0 |
| 8 | 115 | 22 | 0 |
| 9 | 125 | 22 | 0 |
| 10 | 135 | 22 | 0 |
| 11 | 145 | 22 | 0 |
| 12 | 25 | 48 | 315 |
| 13 | 75 | 48 | 45 |
| 14 | 125 | 48 | 0 |
| 15 | 25 | 59 | 315 |
| 16 | 75 | 59 | 45 |
| 17 | 125 | 59 | 0 |
| 18 | 25 | 69 | 315 |
| 19 | 75 | 69 | 45 |
| 20 | 125 | 69 | 0 |
| 21 | 125 | 59 | 270 |
| 22 | 125 | 69 | 270 |
| 23 | 125 | 59 | 90 |
| 24 | 125 | 69 | 90 |

Figure 3. Thermocouple pattern and legend for round filters.

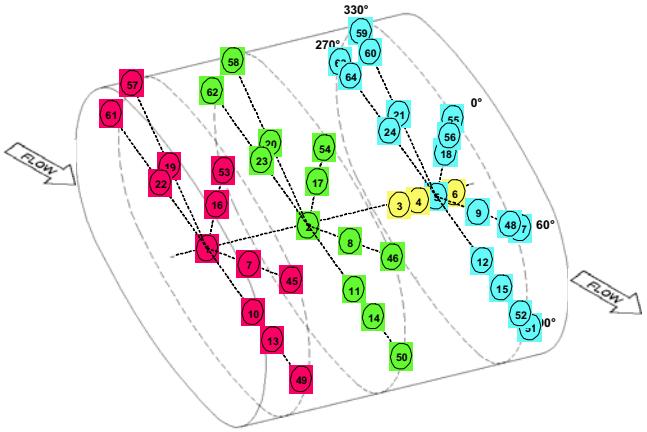


| TC No. | Axial mm | Radial mm | Azimuth deg |
|---|---|---|---|
| 1 | 25 | 0.0 | 0 |
| 2 | 80 | 0.0 | 0 |
| 3 | 130 | 0.0 | 0 |
| 4 | 140 | 0.0 | 0 |
| 5 | 150 | 0.0 | 0 |
| 6 | 160 | 0.0 | 0 |
| 7 | 25 | 40.3 | 60 |
| 8 | 80 | 40.3 | 60 |
| 9 | 150 | 40.3 | 60 |
| 10 | 25 | 46.5 | 90 |
| 11 | 80 | 46.5 | 90 |
| 12 | 150 | 46.5 | 90 |
| 13 | 25 | 66.5 | 90 |
| 14 | 80 | 66.5 | 90 |
| 15 | 150 | 66.5 | 90 |
| 16 | 25 | 26.0 | 0 |
| 17 | 80 | 26.0 | 0 |
| 18 | 150 | 26.0 | 0 |
| 19 | 25 | 40.3 | 330 |
| 20 | 80 | 40.3 | 330 |
| 21 | 150 | 40.3 | 330 |
| 22 | 25 | 46.5 | 270 |
| 23 | 80 | 46.5 | 270 |
| 24 | 150 | 46.5 | 270 |
| 45 | 25 | 80.7 | 60 |
| 46 | 80 | 80.7 | 60 |
| 47 | 150 | 80.7 | 60 |
| 48 | 150 | 70.7 | 60 |
| 49 | 25 | 95.5 | 90 |
| 50 | 80 | 95.5 | 90 |
| 51 | 150 | 95.5 | 90 |
| 52 | 150 | 85.5 | 90 |
| 53 | 25 | 46.0 | 0 |
| 54 | 80 | 46.0 | 0 |
| 55 | 150 | 46.0 | 0 |
| 56 | 150 | 36.0 | 0 |
| 57 | 25 | 80.7 | 330 |
| 58 | 80 | 80.7 | 330 |
| 59 | 150 | 80.7 | 330 |
| 60 | 150 | 70.7 | 330 |
| 61 | 25 | 95.5 | 270 |
| 62 | 80 | 95.5 | 270 |
| 63 | 150 | 95.5 | 270 |
| 64 | 150 | 85.5 | 270 |

Figure 4. Thermocouple pattern and legend for oval filters.

## PRESSURE DROP AND FILTRATION PERFORMANCE

OEMs are concerned about system backpressure which impacts fuel economy. Low filter pressure drop is desirable such that the frequency of regeneration is minimized. Passive regeneration by $NO_2$ oxidation of soot is a means to maintain low soot levels (i.e. low pressure drop). However, soot regeneration by $NO_2$ oxidation requires temperatures above 250 °C and is dependent on NOx/PM ratio [2]. An alternative approach to minimize filter pressure drop as soot accumulates is by filter design. The combination of an asymmetric cell technology filter design and 50% porosity, 15-17 μm MPD has enabled low pressure drop response of AT filters. Certainly, there is a trade-off between low pressure drop and high thermal durability.

### PRESSURE DROP EVALUATIONS

In order to establish clean filter conditions prior to pressure drop evaluations, a controlled regeneration was performed in three steps. First the engine was operated at 2000 rpm, full load for 15 min. to warm up the filter. Then the engine speed was increased to 4000 rpm full load for 1.5 min. to increase exhaust temperature. Finally, post injection was initiated at 1790 rpm/39 Nm for 10 min. A baseline filter clean weight was measured followed by a pressure drop scan. The pressure drop scan consisted of eight operating points as listed in Table 3. The engine speed was increased from 1000 to 4000 rpm to assess the impact of exhaust flow rate at a constant temperature. The last three operating points held the flow rate constant while increasing exhaust temperature.

Table 3. Pressure Drop Engine Operating Conditions

| Engine Speed (rpm) | Engine Torque (Nm) | Duration (sec) |
|---|---|---|
| 1000 | 40 | 30 |
| 1500 | 25 | 30 |
| 2500 | 25 | 30 |
| 2700 | 20 | 30 |
| 3000 | 25 | 30 |
| 4000 | 25 | 30 |
| 4000 | 100 | 30 |
| 4000 | Full Load | 60 |

After completing the pressure drop scan, the filter was cleaned using a controlled regeneration (as described above) and weighed. Then the filter was loaded to 1 g/l soot using a transient cycle to simulate realistic loading conditions on a vehicle. The pressure drop scan followed by filter cleanouts and cumulative soot loadings were repeated for 3 and 6 g/l soot.

The pressure drop of AT ACT 300/13 filters H and I were compared to that of a standard geometry SiC 300/12 filter listed in Table 2. The SiC sample has a higher porosity and median pore size of nominal 59% and 20 μm, respectively, compared to AT. Results in Figure 5 show that AT exhibits a slightly higher clean pressure drop than SiC at 450 $m^3$/h and 200 °C, primarily due to its asymmetric design.

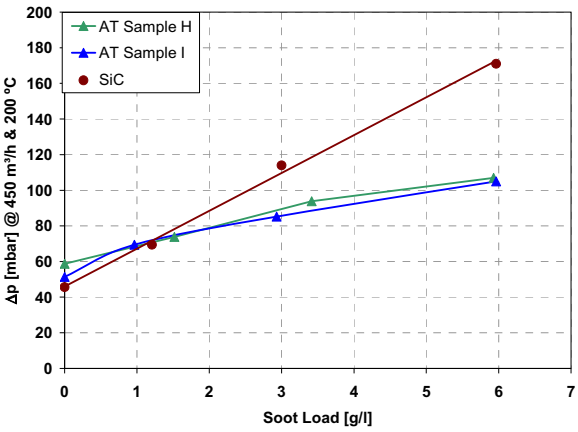


Figure 5. Clean and soot-loaded pressure drop comparison of AT and SiC.

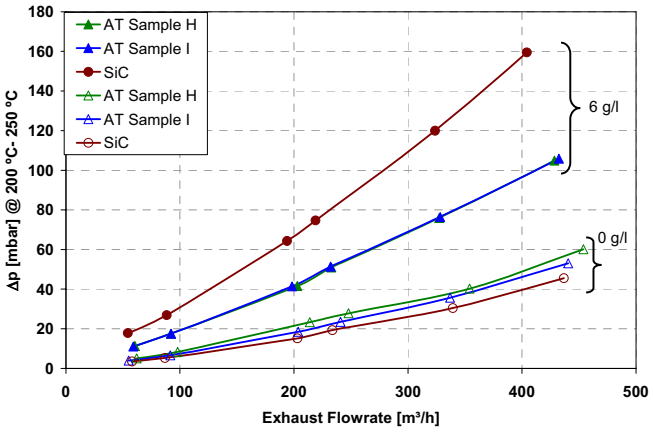


Figure 6. Clean and soot-loaded pressure drop response of AT and SiC with exhaust flow rate.

The variation in clean pressure drop between AT samples H and I is due to slight differences in washcoat loadings. The soot-loaded pressure drop response of AT at 6 g/l soot is 40% lower than SiC. The AT filter can store 2.5 times the soot load as SiC at the same pressure drop level of 100 mbar at 450 $m^3$/h and 200 °C. Significantly lower rise in pressure drop with soot loading is observed for AT than SiC due to the ACT design. Results indicate that the crossover point at which AT exhibits a pressure drop benefit is between 1 - 2 g/l soot load. This soot-loaded dP differential advantage is primarily due to the asymmetric design of AT. The larger inlet channel volume allows a thinner soot layer to be formed on the filter walls. Furthermore, a larger filtration area is provided in the asymmetric design resulting in lower pressure loss than a standard cell wall design.

Comparison of soot-loaded pressure drop with a standard cell structure for AT and SiC also shows a benefit of AT over SiC. The segmentation of SiC filters decreases the open frontal area thereby resulting in higher pressure drop than AT.

As expected, the clean filter pressure drop increases with higher exhaust flow rates. Figure 6 shows higher clean pressure drop response of AT compared to SiC at ~200-250 °C. There is a pressure drop penalty in the clean state for the ACT design due to the contraction and expansion of gases at the filter channel inlet and outlet [1,3] However, a filter spends very little time in a totally clean (fully regenerated) state while in operation on a vehicle. More importantly, the soot-loaded pressure drop dictates filter regeneration intervals and along this point AT demonstrates a significant advantage over SiC.

The soot-loaded pressure drop response exhibits a more pronounced non-linear behavior at higher flow rates compared to a clean filter due to a decrease in the hydraulic channel diameter with soot accumulation. Similar to the clean pressure drop results in Figure 5, sample I displays a lower clean pressure drop than sample H at exhaust flowrates above 100 $m^3$/hr (Figure 6) due to a 5% lower washcoat loading.

## FILTRATION EFFICIENCY PERFORMANCE

On the same VW 2.0l engine used for pressure drop evaluations, filtration performance of designated filters in Table 2 was measured. A cleanout cycle or active regeneration, as described herein above, was conducted following the pressure drop test to remove any residual soot prior to filtration testing. Then smoke measurements upstream and downstream of the DPF were monitored with an AVL 415S smoke meter while operating at the engine conditions listed in Table 4. Filtration efficiency was calculated based on filter smoke number (FSN) measurements before and after the DPF. FSN measurements from two subsequent samplings were used to determine the average filtration efficiency at each operating point.

Table 4. Filtration efficiency operating conditions

| Engine Speed (rpm) | Throttle (%) |
|---|---|
| 4000 | 70 |
| 3500 | 70 |
| 3000 | 100 |
| 2000 | 100 |

Figure 7 compares the filtration efficiency (FE) profile with time for AT and SiC filters as soot accumulates. One data point is plotted every 2 minutes since this is the duration required to capture FSN measurements before and after the DPF.

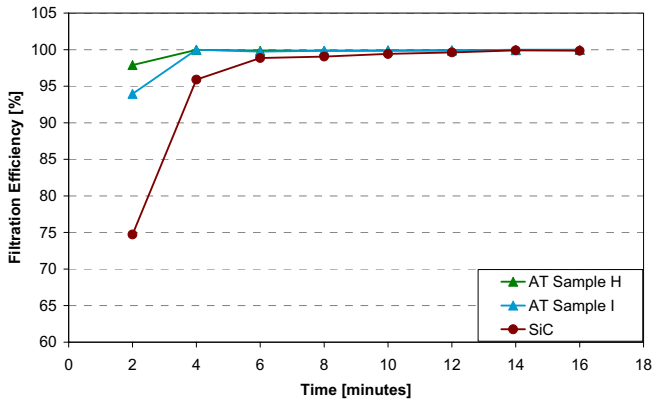


Figure 7. Comparison of AT and SiC filtration performance in clean and soot loaded states.

AT samples H and I exhibit an initial ('clean') filtration efficiency of 98% and 94%, respectively, followed by a rapid increase to 100%. On the other hand, SiC has a lower clean filtration performance of 75% and requires ~12 minutes to achieve 100% FE. The higher nominal 59% porosity and larger 20 μm median pore size of SiC allows more soot penetration through the porous walls than the AT filter during the clean state.

As a soot cake layer forms on the filter walls, it acts to further filter incoming soot; thereby increasing filtration performance. Likewise, buildup of ash generated from lubrication oil provides the same benefit of increased filtration efficiency.

Figure 8 displays average filtration efficiency for AT samples (H and I) and SiC as a function of engine speed stepping from 4000 to 2000 rpm.

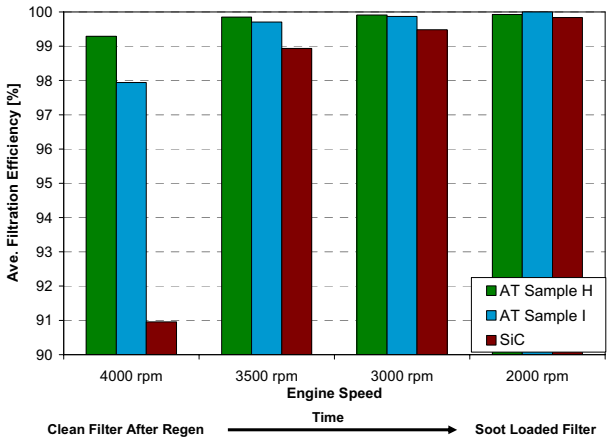


Figure 8. Average filtration performance of AT and SiC at different engine operating conditions.

As previously mentioned the average filtration efficiency is based on two subsequent FSN measurements before and after the DPF.

Results showed a higher average filtration efficiency 4000 rpm for both AT samples compared to the SiC filter. Since the 2nd filtration efficiency value for SiC was >90% compared to the initial low FE (Figure 7), the average initial SiC FE at 4000 rpm was slightly >90%. Less soot penetration is observed for all three filters as engine speed is decreased primarily due to soot buildup on the walls.

## THERMAL SURVIVABILITY PERFORMANCE

### TEST PROCEDURE

Thermal survivability of four AT filters (samples D-G in Table 2.) was evaluated to determine the maximum temperature and maximum gradient a DPF could withstand from a single regeneration event. The filters were soot-loaded on an engine bench to successively higher soot levels followed by regeneration until the filter exhibited signs of failure. Each test cycle at a given soot load increment consisted of soot loading, uncontrolled regeneration, controlled regeneration (cleanout) and integrity check as shown in Figure 9. Soot loading was conducted at steady state conditions of 1470 rpm and 60 Nm achieving a soot output rate of ~8-12 g/hr. The regeneration conditions were chosen to simulate a worst case condition a filter may experience on a passenger vehicle.

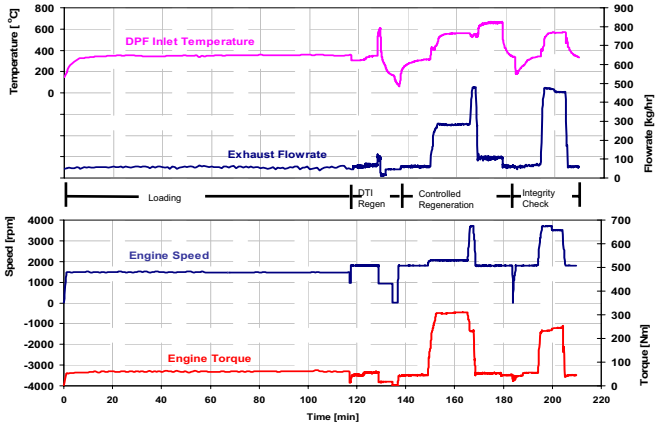


Figure 9. Survivability test cycle and exhaust conditions.

Each cycle consisted of an uncontrolled regeneration where the exhaust inlet filter temperature was stabilized to 330 °C during a 5 min. period of operation at 1800 rpm and 45 Nm. Subsequently, a post-injection pulse (PI) was initiated and maintained until the filter inlet (1" from filter front face) temperature was 640 °C. Then engine speed was dropped to idle (DTI), where the oxygen level increased to facilitate soot combustion and exhaust flow decreased such that heat released was carried away from the filter more slowly. Typically, a filter which undergoes an uncontrolled regeneration

does not achieve complete soot burnout since the inlet filter temperature is not maintained throughout the regeneration. Thus, a controlled regeneration (e.g. cleanout) at higher flow followed by 10 min. of PI was conducted to remove any residual soot. The filter was weighed before and after each regeneration to determine regeneration efficiency and the clean baseline filter weight for the next cycle.

Finally, the filter was checked for possible damage due to previous high temperature exposure during regeneration. The methods used to evaluate filter integrity were visual examination, filter smoke number (FSN), and other nondestructive testing (NDT). The visual check included looking for cracks and soot penetration through the filter. A smoke sweep was conducted consisting of two engine operating points at 4000 and 3500 rpm and full load, where the downstream FSN was monitored for changes in baseline.

## RESULTS

AT samples D-G of similar properties were tested for thermal survivability. As expected, peak filter temperatures generally increase with higher soot loads as shown in Figure 10. Sample D exhibits a shallower slope than other filters. This filter was tested under a less aggressive condition than the other samples with a longer PI duration prior to DTI. The inlet exhaust temperature reached 690 °C prior to DTI for sample D compared to 640 °C for the other filters. In the case of sample D, more soot was regenerated before DTI; thereby resulting in less soot available during idle regeneration and a lower maximum filter temperature.

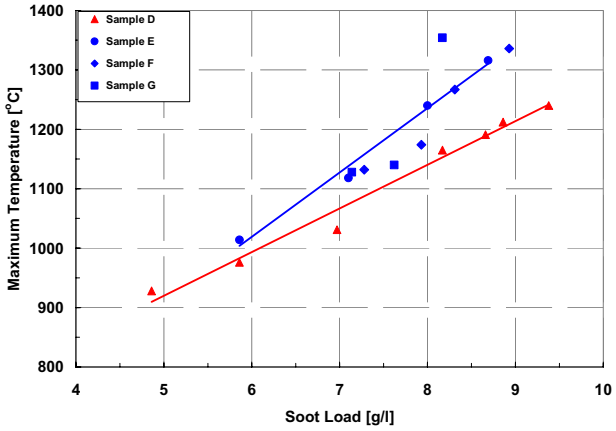


Figure 10. Maximum filter temperatures at various soot loadings during severe DTI testing.

Under the aforementioned regeneration conditions, these AT filters can withstand a single uncontrolled regeneration with soot loadings up to a minimum of 8 g/l. Corresponding maximum temperatures for 8 g/l soot mass limit were in the range of 1200- 1350 °C depending on the post injection period duration before DTI.

Data in Table 5 indicates that the filters tested intentionally to failure limits exhibited small damage with peak temperatures in excess of 1200 °C and maximum radial gradients beyond 600 °C/cm based on the thermocouple pattern in Figure 4. Under typical regeneration conditions on vehicle, the filter will not be exposed to such extreme temperatures with appropriate regeneration control strategies. Due to damage to the peripheral filter channel walls of sample G during thermocouple installation, the largest gradients were not captured.

Table 5. Summary of Survivability Testing Results

| Sample | Soot Load (g/L) | Max. Temperature[a] (°C) | Max. Radial Gradient[a] (°C/cm) | Max. Axial Gradient[a] (°C/cm) | Failure Indicator/ Damage |
|---|---|---|---|---|---|
| D | 9.4 | 1240 | 659 | 240 | PTA[c]/ axial crack |
| E | 8.7 | 1316 | 854 | 401 | FSN & NDT/ axial crack |
| F | 8.9 | 1336 | 768 | 330 | FSN & NDT/ axial crack |
| G | 8.2 | 1354 | 614[b] | 256[b] | Visual & NDT/ axial crack |

[a]Based on thermocouple map in Figure 4. [b]Largest gradients were not measured. [c]Post test analysis – filter dissection.

AT filters exposed to extreme DTI conditions exhibited only axial cracks at the outlet as shown in sample E of Figure 11. No cracks were detected during the survivability test of sample D. Upon dissection during post test analysis, a very fine axial crack was found. Filter damage to sample D was less compared to samples E-G likely due to its less severe regeneration exposures as mentioned above. Although anomalies were found in samples D and G, no impact on FE was observed.

.

Figure 11. Filter sample E outlet end photo after survivability test.

Smoke measurements were successful in detecting cracks during the test which connected inlet and outlet

channels. A small change in smoke number for sample E was observed in Figure 12 at 8.7 g/L soot load where the downstream FSN increased from its baseline level to 0.01. Filter F also exhibited an increase in downstream smoke number at extreme temperatures (> 1300 °C) with 8.9 g/l soot load.

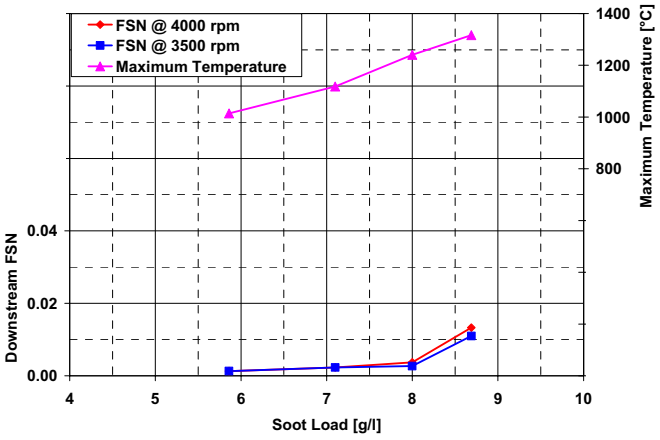


Figure 12. Detection of downstream FSN change of filter sample E during DTI testing.

Nondestructive testing of filters E, F and G showed no indications of radial cracks but, axial cracks were found. Post test analysis results confirmed the absence of radial cracks and the presence of axial cracks for filters D-G.

As a guide for AT filter use on diesel passenger cars, maximum filter temperatures and gradients are identified as limits for successful filter operation based on thermal survivability results. Similarly, others have defined a filter operating map and engine map for filter products based on soot mass limit studies under various engine operating conditions [4]. The maximum temperatures and radial gradients experienced by AT samples D-G during thermal survivability testing are shown in Figure 13. In general, the maximum radial gradient increases as filter peak temperatures increase.

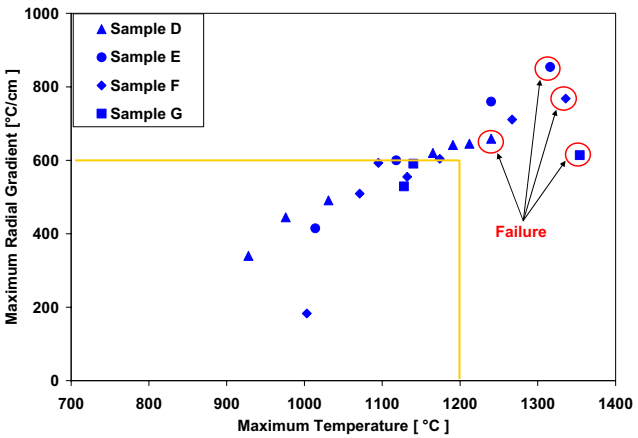


Figure 13. Maximum temperatures and radial gradients of AT filters during thermal survivability evaluations.

Results indicate that no filter failures were observed under the specific uncontrolled regeneration conditions (described above) for filters with maximum temperatures and maximum radial gradients below 1200°C and 600 °C/cm, respectively. All samples failed with exposures >1300 °C except, sample D. Filter cracking is statistical, thus, the probability of cracking increases with maximum temperatures and gradients outside the denoted box in Figure 13. Actual maximum radial gradients for sample G were higher than denoted in Figure 13 but, thermocouple damage to periphery cell walls prevented accurate gradient measurements. Maximum temperatures occurred at the filter outlet at thermocouples 5 or 6 in Figure 4. Maximum radial gradients in the oval filters were observed between thermocouples 55 and 56 or 59 and 60. These maximum gradients occur near the filter skin during regeneration due to heat loss from the thermally conductive surrounding metal can.

These thermal boundary conditions were used as a basis for filter thermal durability studies. The durability evaluations described herein below assess AT performance under multiple high temperature exposures.

## FILTER THERMAL DURABILITY

### CYCLIC REGENERATION RESULTS

Filters durability is a critical parameter to provide indication of a filter's fitness for use in diesel passenger car applications. It is difficult to predict long-term performance except to conduct vehicle tests. An acceptable surrogate test is to conduct engine bench testing to simulate exhaust conditions a filter may experience in the field. The aforementioned survivability test results were used to provide maximum temperature and soot load targets for durability evaluations.

The same test cycle described for survivability testing was used in the durability tests except an additional step was implemented after the filter integrity test. Multiple test cycles of soot load followed by uncontrolled regenerations were performed at a target maximum temperature of 1100 ºC. However, if large variations in the inlet exhaust temperature occur, typically peak exotherms will vary accordingly [5]. Based on the lowest maximum temperature at failure observed during short-term survivability testing (Figure 13), a target peak filter temperature of 1100 ºC was chosen to conduct the longer term durability cycles.

Since weighing the filter after every loading was not practical, the soot load was determined based on the 'apparent resistance', derived from filter pressure drop. By using apparent resistance, the pressure drop is corrected for changes in exhaust temperature and flow rate. A correlation between apparent resistance and soot load was determined during the first few loading cycles by weighing the filter.

DPF samples A-C in Table 2 were tested for thermal durability. The exhaust conditions for a typical uncontrolled regeneration are shown in Figure 14.

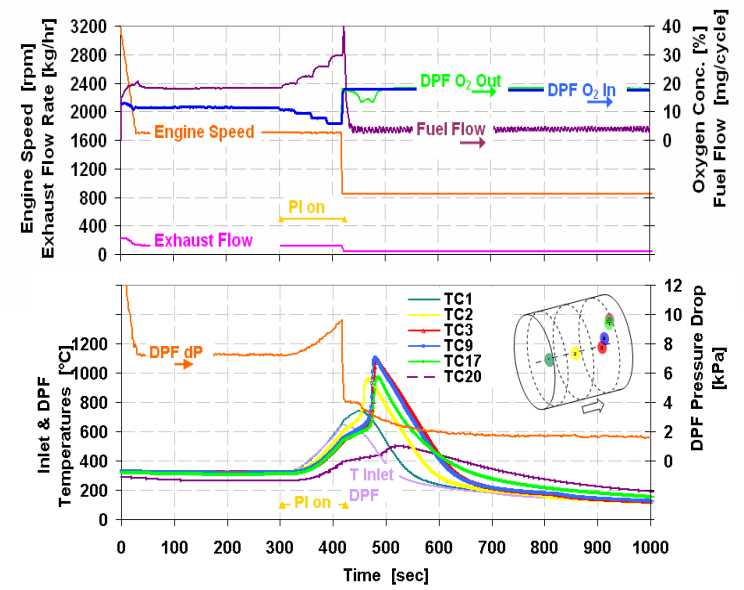


Figure 14. Typical uncontrolled regeneration exhaust (top) and filter (bottom) conditions.

In order to warm up the DPF prior to regeneration, a 5 min. steady state operation at 1700 rpm/3.25 bar BMEP was performed. Then post injection of fuel was initiated in four steps to reach of target inlet temperature of 625 ºC, upon which the engine speed was dropped to idle and post injection terminated. The inlet DPF oxygen concentration decreased as more fuel was injected due to oxidation of hydrocarbons across the upstream DOC. As the flow was decreased from 100 kg/hr to 39 kg/hr at idle, the oxygen concentration into the DPF increased from 6 to 17%. Combustion of soot occurred during idle where an exotherm was generated in the filter and the maximum temperature was observed at the back (thermocouple 9 in Figure 14). As soot was regenerated, incoming oxygen into the DPF was consumed thereby resulting in a drop of oxygen concentration exiting the DPF.

Peak temperatures in the filter increased from front to back as indicated by thermocouples 1, 2 and 3 in Figure 14. The regeneration then propagated from the filter center to the periphery, where heat loss to the environment occurs due to the surrounding conductive metal can. Skin temperatures typically did not exceed 600 ºC in these experiments. The idle condition was maintained for 10 min. which was sufficient for the filter pressure drop and bed temperatures to stabilize.

A summary of the regeneration results for samples A-C is shown in Table 6. Filters were tested from a range of 100 to near 200 high temperature (>1000 ºC) regeneration cycles. Each filter was exposed to double the number of regenerations indicated in the table because each cycle consisted of a controlled regeneration for filter cleanout after the DTI regeneration. The maximum filter temperature observed during each durability test was less than 1250 ºC with maximum gradients not exceeding 650 ºC/cm.

Table 6. Summary of Thermal Durability Regeneration Results

| Sample | No. of Cycles >1000 ºC | Max. Temp. (ºC) | Max. Radial Gradient (ºC/cm) | Max. Axial Gradient (ºC/cm) | Filter Damage |
|---|---|---|---|---|---|
| A | 198 | 1177 | 642 | 416 | None |
| B | 132 | 1240 | 641 | 317 | None |
| C | 101 | 1152 | 593 | 294 | None |

Figure 15 shows the maximum temperatures and thermal gradients of sample C for each cycle. All maximum temperatures and thermal gradients were below 1175 ºC and 600 ºC/cm, respectively. Although half of the regenerations reached high filter temperatures (> 1100 ºC), no filter damaged occurred. Likewise, filters A and B showed no damage upon post mortem dissection although they experienced multiple high temperature exposures. More detailed post mortem results will be described in the next section of this paper.

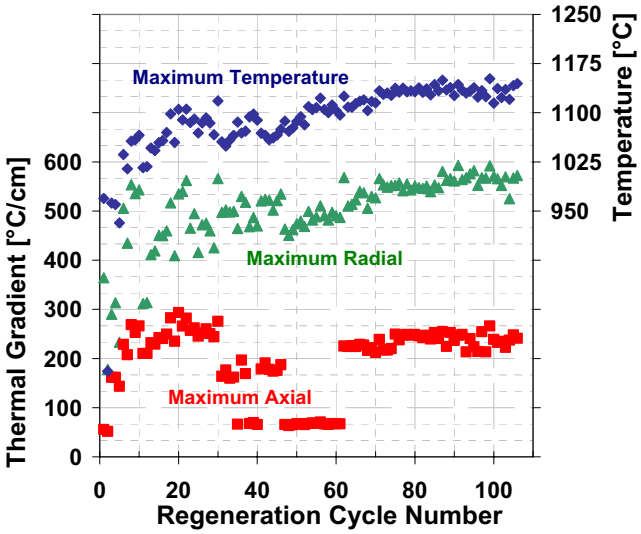


Figure 15. Cyclic regeneration data for sample C.

Maximum temperatures and gradients for sample C were initially low since modest soot loads were used in the initial cycles to confirm filter thermal response during regeneration. Since the skin remains relatively cool during filter regeneration, the largest thermal gradients typically occur in the outermost 1 cm of the filter (i.e. between thermocouples 17 and 20 in Figure 14).

However, maximum axial gradients occur near the filter core at the back where temperatures are the highest during regeneration. Axial gradients for some cycles between 35 and 60 shown in Figure 15 are lower (< 100 ºC/cm) than expected due to failure of thermocouples in key axial positions. Once failed thermocouples were replaced, axial gradients measured between 200 and 300 ºC/cm.

It is estimated that a filter is likely to be exposed to ≤ 600 regenerations over a 240,000 km diesel passenger car life, where < 10% of the regenerations are likely to be uncontrolled. Clearly, AT filters have demonstrated outstanding durability performance by surviving hundreds of uncontrolled regenerations. Likewise, other engine dynamometer and vehicle (> 100,000 km) durability studies of AT have shown that it possesses robustness and durability under severe regeneration conditions.[6,7] The duration of temperature exposure above 1100 ºC for sample A with near 200 uncontrolled regenerations was ~10 minutes as shown in Figure 16.

The expected duration at such high temperatures for filters in passenger car applications is much less. During an uncontrolled regeneration a filter typically experiences peak exotherm for only ~ 30 seconds. The cumulative time above each temperature denoted in Figure 16 was calculated for the four highest temperature thermocouples.

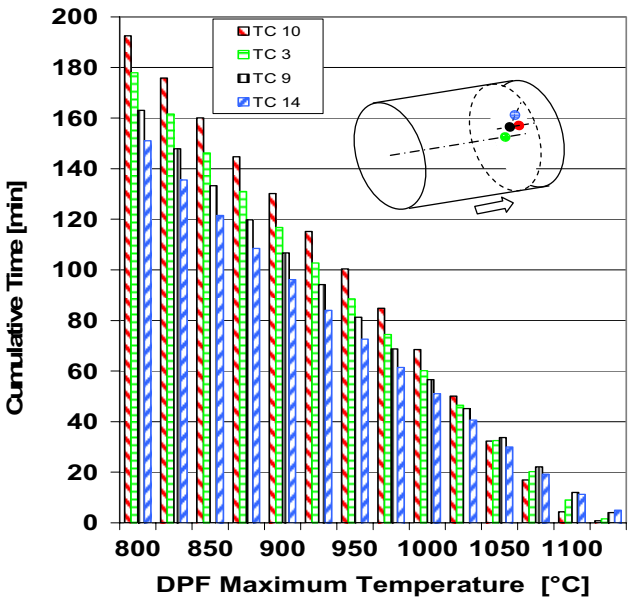


Figure 16. Sample A cumulative time distribution over temperature range.

These thermocouples (3, 9, 10 and 14 in Figure 3) were located at the back-center to back-mid region of the filter. High temperature exposures (>1000 ºC) were the longest at thermocouple 9 or 10 located 22 mm away from the centerline.

## FILTER INTEGRITY EVALUATIONS

Throughout durability testing it was important to monitor filter integrity non-destructively to ensure that the filter had not been damaged by a series of uncontrolled "worst case" regenerations. Following durability testing, the final filter condition was assessed offline by visual inspection and dissection during post test analysis (PTA). During the durability tests, smoke measurements were monitored periodically downstream of the DPF to check for any significant increase from baseline level, which might indicate a loss of filtration performance. Figure 17 shows the downstream FSN values obtained during drop to idle regenerations at 39 kg/hr exhaust mass flow rate. Filtration performance for all AT filters was maintained throughout the high temperature cyclic regenerations. All downstream DPF FSN values were below 0.1, which is the FSN level typically observed for failed or damaged filters under idle conditions on this engine. Results indicate that smoke numbers generally decrease over the durability test likely due to ash accumulation. As ash builds up in the filter it forms a layer on the walls, which helps prevent soot penetration, thereby increasing filtration efficiency. Sample C in Figure 17 shows an increase in smoke number near cycle 100; however the final smoke number is less than the initial baseline value of 0.04. Furthermore, final evaluations of sample C during post test analysis showed no filter damage.

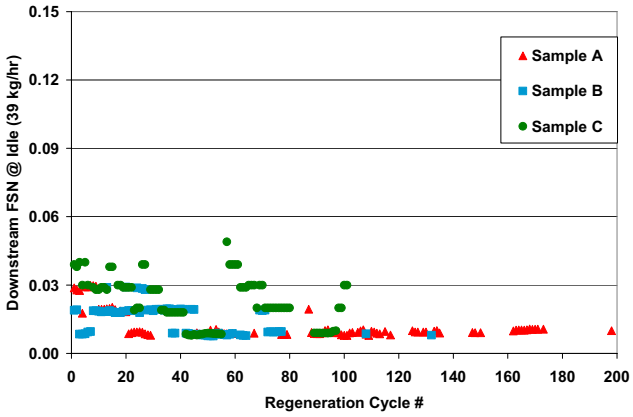


Figure 17. Downstream smoke measurements during uncontrolled regenerations.

Although smoke evaluation was the primary level and most frequent integrity check, other non-destructive tests were used to provide indication about the filter's integrity during the course of the durability test. After 30-50 load/regeneration cycles were completed on a filter, it was evaluated for cracks using non-destructive techniques as secondary measures. These intermittent non-destructive evaluations indicated that filters A-C had no signs of damage. Furthermore, evaluations performed during destructive filter PTA confirmed the absence of cracks for samples A-C.

After completion of engine durability tests, filters A, B and C were submitted for post test analysis which includes dissection, further analysis for any internal damage, and physical property evaluations. Figure 18 shows photos of both halves of the samples after dissection and no damage was observed in any of the filters. The variation in color from inlet to outlet denotes zone coating of the filters. These halves were cut further axially and radially to check for damage and none was found.

| Sample | PTA Photo |
|---|---|
| A | 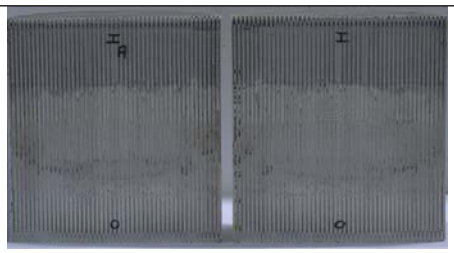 |
| B | 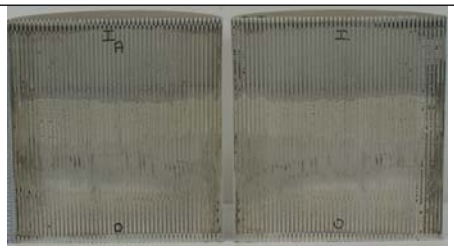 |
| C | 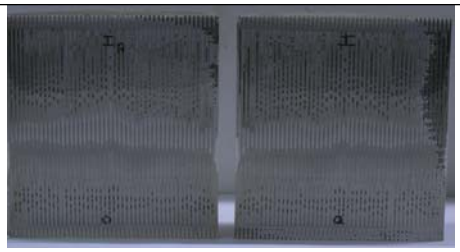 |

Figure 18. Summary of durability filters integrity results – photographs of filter halves after dissection.

Since a passenger car is expected to be in use for 240,000 km with a regulated filter life of 160,000 km, the filter material must not only be thermo-mechanically durable but, thermodynamically stable and chemically resistant to components in the exhaust such as soot, ash, moisture, and acid. A previous paper has described AT's excellent chemical resistance against such exhaust components [8]. Typically ash begins to adhere to aluminum oxide filters and sinter at temperatures above 1100 ºC [8,9]. However, temperatures in excess of 1300 ºC are required before any significant interaction of ash with aluminum titanate material matrix was observed. [9]

Previous studies have shown that long term exposure (on the order of hours) of aluminum titanate to 1100-1200 ºC under reducing or oxidizing conditions is likely to result in decomposition forming alumina and titania [10]. This decomposition is most easily detected by a significant increase in the thermal expansion coefficient (CTE). However, stabilizing additives can significantly slow down this reaction [10,11]. The AT filter composition described herein has been stabilized to eliminate the possibility of decomposition even under extreme DPF exposures. Furthermore, filter exposure to temperatures in this regime is on the order of several minutes during diesel passenger car lifetime.

The goals of the durability study discussed in this paper were to evaluate the thermo-mechanical durability and thermodynamic stability of AT filters under high temperature reducing and oxidizing conditions. The impact of engine aging on filter thermo-mechanical durability and thermodynamic stability of AT was evaluated by comparison of fresh (unaged) filter properties to the durability aged filter properties. Thus the filter halves of the durability samples were dissected further to obtain samples for physical properties evaluation.

A key measure used to describe filter thermal durability is the thermal shock parameter (TSP) which depends upon the material modulus of rupture (MOR), CTE, and elastic modulus (Emod) as indicated in equation 1 [5].

$$TSP\ (ºC) = MOR/(CTE * Emod) \qquad [1]$$

For good thermal shock resistance, a filter should exhibit high MOR, low CTE and low Emod. The baseline axial MOR, CTE and Emod for coated control (unaged) filters are indicated by the open symbols at the 100% level in Figure 19.

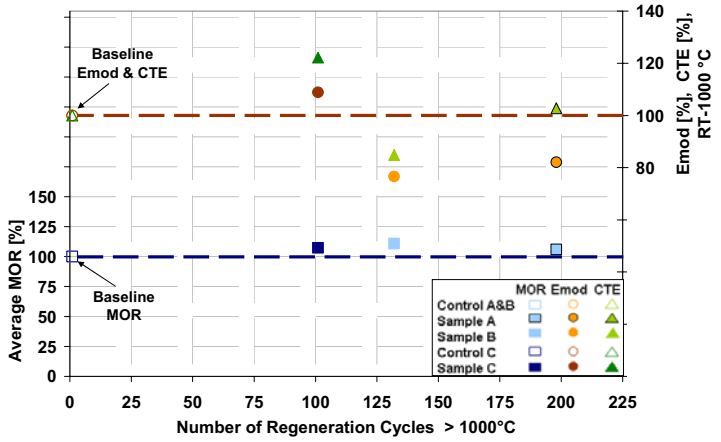


Figure 19. Axial MOR, CTE and Emod results for coated fresh (control) and coated engine aged durability samples.

The two control samples (Control A&B and Control C) are sister samples (exposed to the same firing) to the corresponding durability aged test samples. These control samples have experienced one regeneration for

filter conditioning purposes. The average axial MOR for each sample represents ten MOR measurements. Compared to the baseline MOR strength, all aged samples showed an increase in strength of 6-11%.

The axial CTE was measured from room temperature to 1000 ºC at the outlet end of the filter where temperatures were the highest. Results indicated that after filter aging, samples B and C varied by ~20% in CTE with respect to baseline. However, the resultant change in CTE translated into a one point difference from baseline for samples B and C. Sample A showed no change in CTE compared to baseline. Also, no change in the x-ray diffraction (XRD) pattern for all samples was observed after the durability tests. Thus, CTE and XRD results provide conclusive evidence that the AT filter shows no signs of decomposition with engine aging.

Finally, a ~20-25% decrease in axial Emod with aging was observed for samples A and B, which suggests an improvement in thermal shock resistance given the noted increase in MOR and no significant change in CTE. Sample C shows a 9% increase in Emod after 100 cycles compared to control C baseline Emod. However, this modest increase in Emod and CTE did not result in any physical damage to filter sample C. The physical property results and PTA evaluations indicate that the excellent thermal shock resistance of AT filters is maintained after engine aging under the aforementioned operating conditions. AT filters have demonstrated outstanding durability performance by surviving hundreds of high temperature exposures with no significant negative impact on physical properties.

## CONCLUSION

The new Corning AT filter has shown its excellent thermal durability by withstanding peak temperatures and thermal gradients up to 1200 °C and 600 °C/cm, respectively for a single regeneration. Due to their outstanding thermal shock resistance, AT filters have survived high temperature exposures in excess of 100 cycles with no evidence of filter damage. Furthermore, comparison of physical properties before and after durability testing showed no negative impact on thermo-mechanical durability.

The tailored microstructure and asymmetric cell design of AT filters provide a lower soot-loaded pressure drop than commercially available SiC, with slightly higher clean pressure drop. The lower soot-loaded pressure drop will enable higher fuel economy with less frequent regenerations. Furthermore, the asymmetric cell geometry allows higher ash storage capacity than a standard wall configuration. Thus, lower pressure drop is observed and smaller filters can be utilized to minimize space for the emissions system. In addition AT demonstrates higher mass-based filtration performance than SiC in a clean state. As a soot layer accumulates on the filter wall, the filtration efficiency of AT reaches 100% more rapidly than SiC.

## ACKNOWLEDGMENTS

The authors wish to thank Mr. Tom Giamichele, Mr. Seth Goodreau, and Ms. Susan Stage-Derick for processing the samples, and Mrs. Connie Sawyer, Mrs. Holly Gray, Tom Averill, and Chris Hill for post test analysis evaluations. We also wish to thank members of Corning Incorporated Characterization Services for physical properties measurements.

## REFERENCES

1. Young, D. M., Hickman, D. L., Bhatia, G. and Gunasekaran, N., “Ash Storage Concept for Diesel Particulate Filters”, SAE 2004-01-0948.
2. Soeger, N., Mussmann, L., Sesselmann, R., Leippe, G., Gietzelt, C., Bailey, O. and Hori, M., “Impact of Aging and NOx/Soot Ratio on the Performance of a Catalyzed Particulate Filter for Heavy Duty Diesel Applications”, SAE-2005-01-0663.
3. Konstandopoulos, A. G., Skaperdas, E., and Masoudi, M., “Inertial Contributions to the Pressure Drop of Diesel Particulate Filters”, SAE 2001-01-0909.
4. Locker, R. J., Sawyer, C. B., Menon, S., Floerchinger, P. and Craig, A. G., “Diesel Particulate Filter Operational Characterization”, SAE 2004-01-0958.
5. Locker, R.J., Gunasekaran, N. and Sawyer, C., “Diesel Particulate Filter Test Methods”, SAE 2002-01-1009.
6. Heibel, A. K., Schultes, J. A., Bhargava, R. Y., Boger, T., Rose, D., Pittner, O., “Performance and Durability Evaluation of the New Corning DuraTrap® AT Diesel Particulate Filter – Results from Engine Bench and Vehicle Tests”, Aachener Kolloquium Fahrzeug-und Motorentechnik”, 14, 2005.
7. Boger, T., Rose, D., Cutler, W. A., Heibel, A. K., Tennent, D. L., “Evaluation of New Diesel Particulate Filters Based on Stabilized Aluminum Titanate”, MTZ, 2005.
8. Ogunwumi, S. B., Tepesch, P. D., Chapman, T., Warren, C. J., Melscoet-Chauvel, I. M., and Tennent, D. L., “Aluminum Titanate Compositions for Diesel Particulate Filters”, SAE 2005-01-0583.
9. Merkel, G.A., Cutler, W.A. and Warren, C.J., “Thermal Durability of Wall-Flow Ceramic Diesel Particulate Filter”, SAE 2001-01-0190.
10. Freudenberg et al, US Patent # 5,153,153, Oct. 6th 1992.
11. G. Tilloca, Journal of Material Science, 26 (1991) 2809-2814.